# EVALUATION OF $Y_2O_3$ AS FRONT LAYER OF CERAMIC CRUCIBLES FOR VACCUM INDUCTION MELTING OF TiAl BASED ALLOYS

Joaquim Barbosa[1], C. Silva Ribeiro[2], O.M.N.D. Teodoro[3], Caetano Monteiro[1]

[1]Universidade do Minho, Departamento de Engenharia Mecânica
Azurém, 4800 Guimarães, Portugal
[2]FEUP, Departamento de Engenharia Metalúrgica e de Materiais
Rua Roberto Frias, 4200-465 Porto, Portugal
[3]CEFITEC, Departamento de Física da Faculdade de Ciências e Tecnologia
Universidade Nova de Lisboa, 2829-516 Caparica

Keywords: TiAl, Induction Melting, Ceramic Crucible

## Abstract

During the last decades titanium alloys were found to be valuable engineering materials for many different applications. Formerly used in critical applications like aerospace, aeronautic and military equipment, where the factor cost is not relevant, titanium alloys are finding now new and different markets.

However, the development of such new markets will depend on an effective cost reduction of titanium parts, in order to achieve a selling cost suitable with its application in consumer goods. A possible solution to decrease production costs might be the use of traditional casting techniques to produce near net shape functional parts. During the last years, the authors have developed extensive research work on this field, and a new technique both for melting and moulding, using ceramic multi-layered crucibles and investment casting shells was developed. This paper presents some of the results obtained during that research work: Ti-48Al alloy were melted and cooled inside CaO, MgO and $Y_2O_3$ stabilized $ZrO_2$ crucibles with inside layer of $Y_2O_3$. The chemical composition, hardness and microstructure at the metal-crucible interface, studied by secondary ion mass spectrometry, SEM/EDS and XRS are presented. On a second step, the same alloy was melted on the same crucibles, and poured into graphite moulds, and the crucibles wall was characterized by SEM/EDS and XRS.

## Introduction

Foundry is one of the technologies available to process titanium alloys. However, the high reactivity of those alloys with almost every element makes very difficult the use of traditional casting techniques and equipment to obtain sound castings. For such reason, specially designed furnaces (cooled copper crucible induction or arc furnaces) are used for vacuum melting pre-prepared (by multiple remelting) melting charges with the desired chemical composition, and the molten metal is poured in ceramic moulds obtained by the investment casting process. In many cases, the molten alloy is poured in the form of billets that are postly processed by forming in order to obtain approximate final shapes. The present processing technology often

573

leads to castings with a surface hard-case, usually called "alpha-case", due to the presence of contaminants on that region, mainly oxides, that must be removed by chemical milling. For such reasons, titanium alloys parts are extremely expensive, and its use is limited to special and critical applications where the factor cost is almost irrelevant, like in the aerospace, aeronautical or military industries.

During the last years, an effort to develop a casting technique suitable to produce Ti based castings at competitive cost, based on the traditional ceramic crucible induction melting technique, has been done by several researchers, where the authors are included. Results obtained so far show that no material accomplishes the melting crucibles two main demands: inertness facing the titanium alloy and high thermal-shock resistance. Due to the high reactivity of such alloys, no material has been found absolutely inert facing titanium, and the yttrium and calcium oxides were found to be those chemically more stable when used as crucible materials [1-8]. However, in both cases, the crucibles thermal-shock resistance was found to be poor, and there are references to crucibles that cracked during melting. Besides, calcium oxide reveals manipulation problems, due to its high higroscopicity.

The crucibles thermal-shock resistance can be improved if partially or fully stabilized zirconium dioxide is used on its production. However, its reactivity with molten titanium alloys is higher, and its use usually leads to the contamination of the alloys with Zr and O [1,4,5,8]. Finally, the extremely high cost of those refractories, mainly in what concerns $Y_2O_3$, makes its use on the production of ceramic crucibles almost forbidden.

Facing such results, the authors developed a two-layer ceramic crucible to be used to melt TiAl. In order to grant the desired thermal-shock resistance and an affordable cost, crucibles are based on stabilized $ZrO_2$, and present an $Y_2O_3$ inside layer in order to achieve the desired chemical stability facing TiAl, and so decreasing the probability of a metal-crucible interaction to occur. Results obtained using the developed technique are quite satisfactory, and very low contaminated castings were produced, revealing no "alpha-case" and excellent surface finishing.

## Experimental Technique

### Melting operation

Ti-48Al alloys have been produced, prepared from pure aluminium and titanium, melted in multi-layer crucibles. $ZrO_2$ crucibles partially stabilized with $Y_2O_3$, MgO and CaO were used as base crucibles, in order to study the influence of the stabilizer compound on the crucible thermal-shock resistance. Every crucible was inside coated with an $Y_2O_3$ film 200 μm thick, in order to achieve the desired chemical stability.

Melting was performed on an induction furnace, inside a sealed chamber, where a controlled atmosphere of commercial pure argon was maintained. The melting procedure was the same as used in previous work and published elsewhere [1,5]. Melting stock weights 100 g, made of titanium rod grade II and commercial pure 99,8% aluminium. In order to evaluate the effect of a slower cooling rate upon the residual element content, the melts have been allowed to solidify and cool inside the melting crucible until room temperature. Some melts have been

centrifugally poured into graphite moulds, to allow the evaluation of the crucible wall after melting. Melting temperature was 1600ºC

Samples characterization

Cast specimens obtained by letting the alloy to solidify inside the melting crucible were cylinders 40 mm in diameter and 22 mm long. Samples for characterization were collected from the middle section of them, by cutting the cylinders at half their height, and prepared using traditional metallographic techniques.

Samples characterization includes microstructure identification, chemical composition and microhardness values of each microconstituent, and "alpha-case" characterization. Chemical composition measurement was performed by quantitative EDS analysis with standards of pure Ti, Al, Zr and Y, using a JEOL JSM 35C scanning electron microscope. Overall oxygen content was measured using the Inert Gas Fusion (IGF) technique. Oxygen content variation from the surface to the inside of samples was evaluated by Secondary Ion Mass Spectroscopy (SIMS). SIMS has been performed in a Multitechnique Surface Analysis System detailed described elsewhere [9]. A 4 keV $Ar^+$, 200 nA beam focused in a 50µm diameter was used. Secondary ions produced by sputtering where mass analyzed by a quadrupole type mass spectrometer. Both positive and negative spectra were taken. Base pressure during analysis was in the order of $10^{-9}$ mbar. X-Ray diffraction was used to identify compounds present on the microstructure. Microhardness was evaluated on a Shimadzu hardness tester, using a 50g load, for 15 seconds.

# Experimental Results

Samples microstructure

As shown in Figure 1, the microstructure is very similar for every sample, no matter the crucible used to produce them: a lamellar dendritic constituent with two phases ($\alpha_2 + \gamma$) and an interdendritic $\gamma$ phase. The lamellar constituent is present on a volume fraction of around 80% that increases from the samples surface to the inside, following the decrease of the cooling rate. Every sample reveals the presence of small inclusions that the EDS spectrum (Figure 2 c)) suggests to be yttrium oxide.

Microconstituents were identified through its chemical analysis (Table I) and EDS spectrum (Figure 2), and later confirmed by X-Ray Diffraction (Figure 3). The same X-Ray Diffraction evaluation proves that the small inclusions are in fact $Y_2O_3$ particles which origin is believed to be the erosion of the $Y_2O_3$ film present on the crucible interior wall. When compared with samples produce before in single $Y_2O_3$ stabilized $ZrO_2$ crucibles (Figure 1 d)) [1], the presence of aluminum oxide is not detected, what suggests the high chemical stability of the $Y_2O_3$ inside layer.
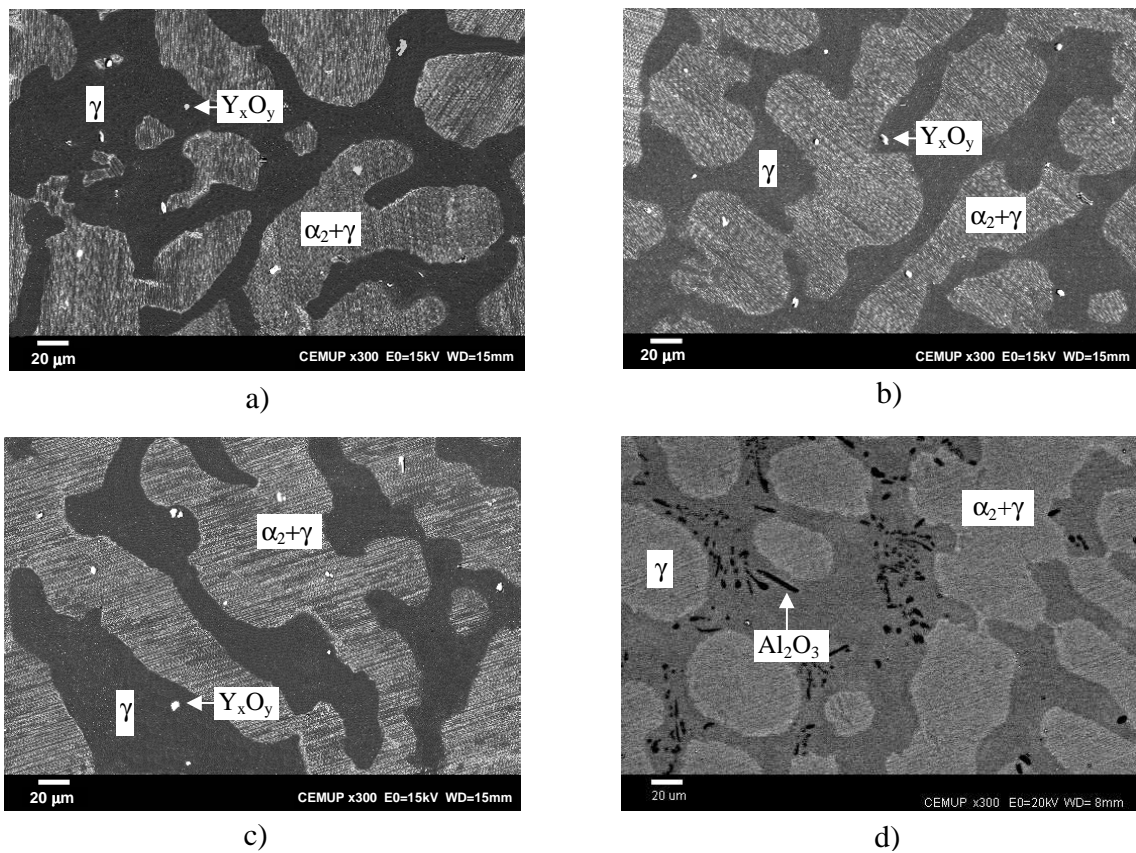
Figure 1. Microstructure of Ti-48Al cast samples obtained on partial stabilized $ZrO_2$ crucibles using a) $Y_2O_3$, b) MgO and c) CaO as stabilizing compounds, inside coated with a $Y_2O_3$ film. Microstructure d) respects to a cast sample of the same material obtained in single $Y_2O_3$ stabilized $ZrO_2$ crucible [1].
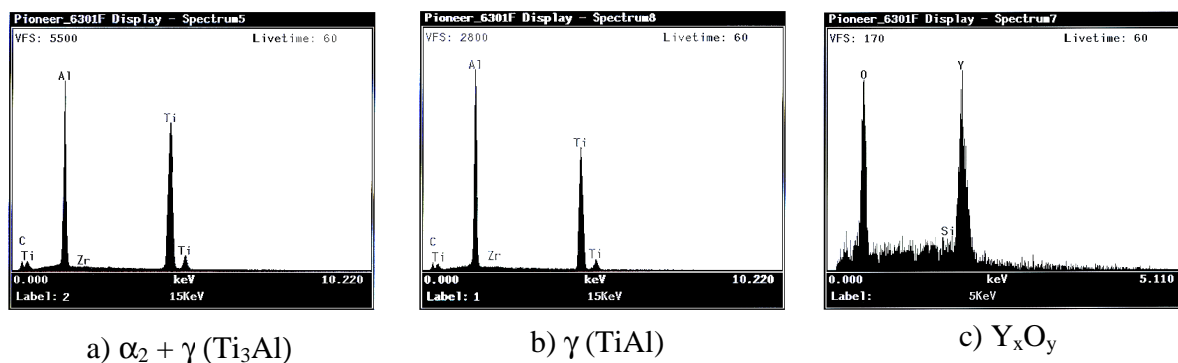


Figure 2. EDS spectrum of the constituents present on the microstructure of the sample obtained in $Y_2O_3$ partially stabilized $ZrO_2$ crucibles with inside $Y_2O_3$ layer.
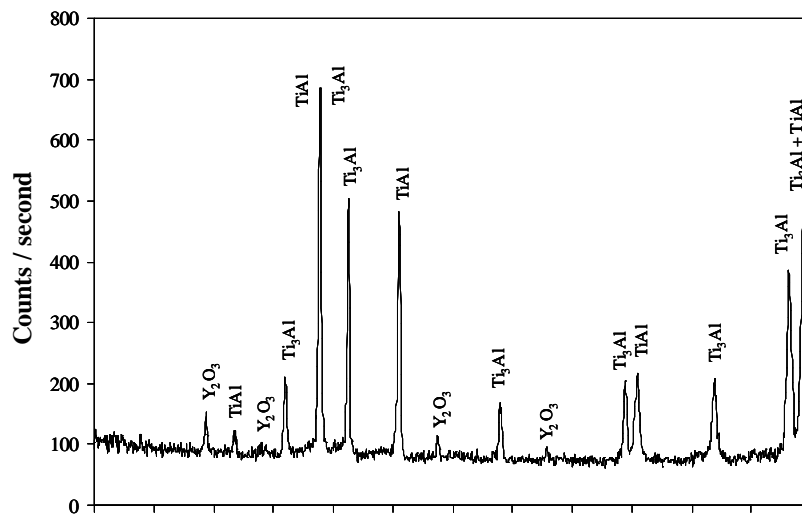
Figure 3. X-Ray Diffraction spectrum of the sample obtained in $Y_2O_3$ partially stabilized $ZrO_2$ crucibles with inside $Y_2O_3$ layer, showing the co-existence of $Ti_3Al$, $TiAl$ and $Y_2O_3$.

Chemical composition

Concerning the chemical composition, the lamelar $\alpha_2 + \gamma$ constituent has higher Ti content (51,8 – 54,9 at%) and the $\gamma$ interdendritic phase higher Al content (51,7 – 54,8 at%), in every produced sample (Table I), which is in accordance with the available references. Every sample reveals a slight contamination with Y (average value between 0,14 and 0,16 at%) (Table I), that dissolves in both microconstituents, although a little more in the lamellar one. In every sample Y concentration is higher at the surface (0,23 – 0,28 at% on $\alpha_2 + \gamma$, at a distance to the surface of 25 $\mu$m, and 0,17 – 0,22 at% on the $\gamma$ phase, at a distance to the surface of 50 $\mu$m), and it decreases to the inside of sample until reaching the average values referred in Table I.

The Y content of the interstitial $\gamma$ phase at 25 $\mu$m from the samples surface is not available, as its volume fraction is very small at that area, and the chemical analysis could not be done according to the standards. The presence of Zr in solution was not detected, revealing an effective isolation of the crucibles base material by the $Y_2O_3$ layer.

The O overall content of the samples measured using the IGF technique is 0,31 wt% on samples obtained in multi-layer $Y_2O_3$ and CaO stabilized $ZrO_2$ based crucibles, and 0,29 wt% on sample obtained in MgO stabilized ones. Assuming that the O content of the alloy, due to the melting charge constituents is around 0,16 wt%, the entire processing results on an O concentration increase between 0,13 and 0,15 wt%. This value is significantly lower than references of Saha [8] (0,85 wt%) and Richerson [10] (0,5 wt%) for laboratory experiments simulating the casting process, using $Y_2O_3$ as ceramic material and commercially pure Ti and Ti-Be alloys as molten alloys, respectively.

Table I. Chemical analysis of samples obtained in $Y_2O_3$, MgO and CaO stabilized $ZrO_2$ crucibles, with inside layer of $Y_2O_3$.

| Depth from surface (µm) | | 25 | 50 | 75 | 100 | 200 | 300 | 500 | bulk |
|---|---|---|---|---|---|---|---|---|---|
| **Constituent** | **Element** | **Chemical composition (at%)** | | | | | | | |
| **Crucible: $ZrO_2/Y_2O_3 + Y_2O_3$** | | | | | | | | | |
| $\alpha_2 + \gamma$ | Ti | 53,0 | 52, 8 | 53,8 | 53,1 | 53,3 | 53,0 | 52,4 | 53,5 |
| | Al | 46,7 | 47,0 | 46,1 | 46,7 | 46, 6 | 47,9 | 47,6 | 46,3 |
| | Y | 0,25 | 0,22 | 0,13 | 0,15 | 0,14 | 0,10 | <0,1 | 0,16 |
| | Zr | - | - | - | - | - | - | - | - |
| $\gamma$ | Ti | n.a. | 46,4 | 46,9 | 45,1 | 46,7 | 46,9 | 48,2 | 46,9 |
| | Al | n.a. | 53,4 | 53,0 | 54,8 | 53,2 | 53,1 | 51,7 | 52,9 |
| | Y | n.a. | 0,17 | 0,13 | 0,13 | 0,12 | <0,1 | 0,13 | 0,13 |
| | Zr | n.a. | - | - | - | - | - | - | - |
| Average composition (at.%)   Ti – 52,22   Al – 47,62   Y – 0,16 | | | | | | | | | |
| **Crucible: $ZrO_2/MgO + Y_2O_3$** | | | | | | | | | |
| $\alpha_2 + \gamma$ | Ti | 53,8 | 54,1 | 53,4 | 54,9 | 54,3 | 54,1 | 53,8 | 53,5 |
| | Al | 46,0 | 46,6 | 46,4 | 45,0 | 45,7 | 46,8 | 46,1 | 46,3 |
| | Y | 0,23 | 0,25 | 0,15 | 0,13 | <0,1 | 0,13 | <0,1 | 0,14 |
| | Zr | - | - | - | - | - | - | - | - |
| $\gamma$ | Ti | n.a. | 46,8 | 48,2 | 47,3 | 46,9 | 47,9 | 47,3 | 47,3 |
| | Al | n.a. | 53,0 | 51,7 | 52,5 | 52,9 | 52,0 | 52,6 | 52,6 |
| | Y | n.a. | 0,19 | 0,14 | 0,13 | < 0,1 | <0,1 | 0,12 | 0,13 |
| | Zr | n.a. | - | - | - | - | - | - | - |
| Average composition (at.%)   Ti – 52,11   Al – 47,75   Y – 0,14 | | | | | | | | | |
| **Crucible: $ZrO_2/CaO + Y_2O_3$** | | | | | | | | | |
| $\alpha_2 + \gamma$ | Ti | 52,7 | 53,7 | 51,8 | 53,1 | 52,8 | 52,9 | 52,7 | 53,3 |
| | Al | 47,0 | 46,1 | 48,0 | 46,8 | 47,1 | 47,0 | 47,1 | 46,5 |
| | Y | 0,28 | 0,26 | 0,15 | 0,14 | 0,13 | <0,1 | 0,15 | 0,15 |
| | Zr | - | - | - | - | - | - | - | - |
| $\gamma$ | Ti | n.a. | 46,5 | 46,9 | 47,8 | 46,5 | 47,1 | 46,4 | 47,4 |
| | Al | n.a. | 53,3 | 53,0 | 52,1 | 53,5 | 52,8 | 53,5 | 52,5 |
| | Y | n.a. | 0,22 | 0,14 | 0,12 | < 0,1 | 0,13 | 0,10 | 0,12 |
| | Zr | n.a. | - | - | - | - | - | - | - |
| Average composition (at.%)   Ti – 52,53   Al – 47,32   Y – 0,15 | | | | | | | | | |

In every sample, the oxygen content decreases from the casting surface to the inside, as represented in Figure 4 for a sample obtained in multi-layer $Y_2O_3$ stabilized $ZrO_2$ based

crucibles. The O concentration profile is irregular, but almost constant, for distances to the samples surface less than 80 μm, and becomes lower and irregular, but also almost constant, for higher distances.
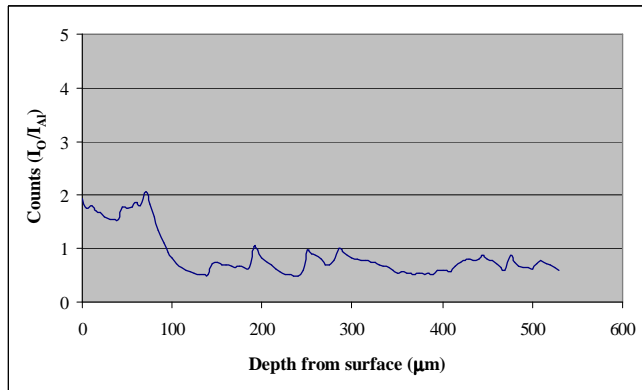


Figure 4. Oxygen concentration profile from the surface to the inside of a sample obtained in $Y_2O_3$ partially stabilized $ZrO_2$ crucibles with inside $Y_2O_3$ layer, showing the presence of higher values in regions close to the

Microhardness

Table II presents the microhardness values for each microconstituent, at different distances from the samples surface. Inside the samples microhardness values are between 306 and 311 HV in the $\alpha_2+\gamma$ constituent and between 289 and 296 HV in the interdendritic $\gamma$ phase, which is in accordance with available references. A slight increase in microhardness at distances from surface less than 100 μm can be detected on the $\alpha_2+\gamma$ constituent, which is due to the increase of oxygen content on that area. The effect of oxygen in the hardness of the interdendritic $\gamma$ phase is not detected, as its solubility on that phase is lower than 0,06 wt% [11].

Table II – Microhardness variation profiles on each microconstituent, from the surface to the inside of Ti-48Al samples obtained in $Y_2O_3$, MgO and CaO stabilized $ZrO_2$ crucibles, with inside layer of $Y_2O_3$.

| Depth from surface (μm) | 50 | 100 | 200 | 300 | 500 | 1000 | bulk |
|---|---|---|---|---|---|---|---|
| **Constituent** | **Microhardness (HV)** | | | | | | |
| **Crucible: $ZrO_2/Y_2O_3 + Y_2O_3$** | | | | | | | |
| $\alpha_2 + \gamma$ | 319 | 313 | 306 | 311 | 309 | 306 | 311 |
| $\gamma$ | - | 289 | 296 | 301 | 289 | 296 | 296 |
| **Crucible: $ZrO_2/Y_2O_3 + Y_2O_3$** | | | | | | | |
| $\alpha_2 + \gamma$ | 316 | 311 | 301 | 306 | 303 | 303 | 306 |
| $\gamma$ | - | 296 | 293 | 296 | 293 | 296 | 296 |
| **Crucible: $ZrO_2/Y_2O_3 + Y_2O_3$** | | | | | | | |
| $\alpha_2 + \gamma$ | 316 | 311 | 306 | 303 | 309 | 306 | 309 |
| $\gamma$ | - | - | 301 | 296 | 289 | 303 | 289 |

Metal-crucible interface

Figure 5 shows the microstructure of the surface (metal-crucible interface) of a sample obtained in a $Y_2O_3$ partially stabilized $ZrO_2$ crucible with inside $Y_2O_3$ layer.



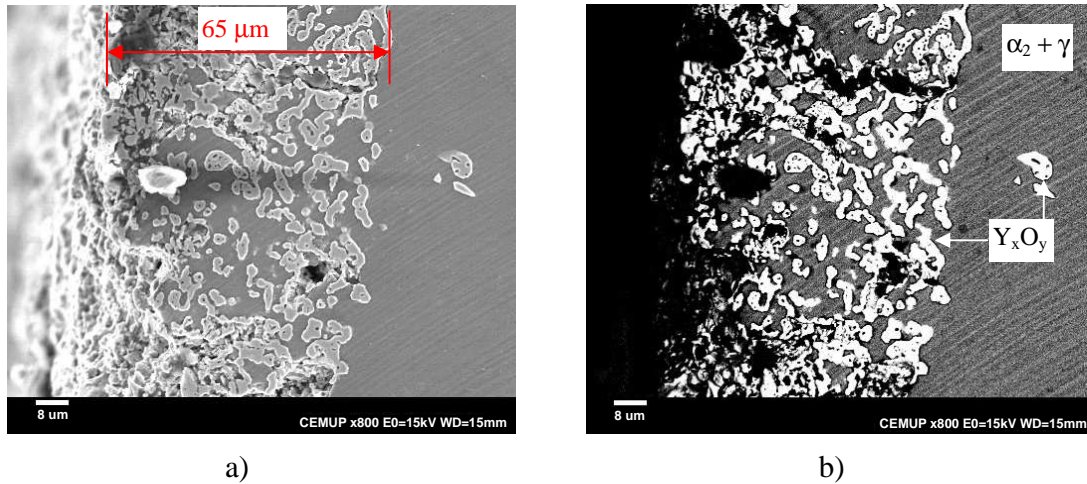a)                                                              b)

Figure 5. Microstructure of the surface (metal-crucible interface) of a Ti-48Al sample obtained in a $Y_2O_3$ partially stabilized $ZrO_2$ crucible with inside $Y_2O_3$ layer. The matrix lamellar structure is easily seen in figure b), as well as an yttrium oxide layer about 65 µm thick.

A layer of dispersed grains can be seen at the sample surface over a $\alpha_2+\gamma$ lamellar matrix that the EDS spectrum revealed to be yttrium oxide particles (Figure 6). The presence of yttrium oxide particles at the casting surface, as well as on the bulk as already referred, suggests that an erosion phenomena of the crucible $Y_2O_3$ layer occurred. Although no microstructure significant alteration was found at the interface, besides the decrease of the volume fraction of the interdendritic $\gamma$ phase, to suggest any kind of metal-crucible reaction. However, the presence of Y and O in the alloy reveals that some kind of interaction occurred, suggesting that the $Y_2O_3$ layer was dissolved, or slightly reduced by the alloy, what is in agreement with Saha references [8].

These phenomena might explain the O and Y concentration profiles found in samples chemical composition. During the molten state, the liquid metal slightly dissolves the Y2O3 layer, which results in a uniform distribution of those elements in the metal, due to the induction heating stirring effect and high diffusion rates. When heating is stopped, dissolution continues, but O and Y diffusion rates become slower and a composition gradient starts to form from the surface to the inside of samples.

The presence of titanium oxides, namely TiO and $TiO_2$, as a consequence of the presence of high oxygen content at the metal-crucible interface was not detected, but its presence during

processing can not be excluded. In fact titanium oxides dissolve easily in liquid titanium [12], and as a consequence, its presence would be very difficult to detect.
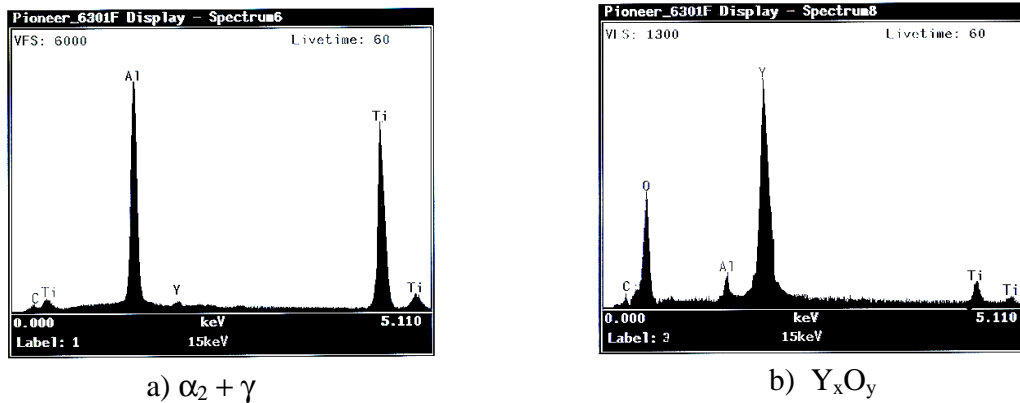


a) $\alpha_2 + \gamma$            b) $Y_xO_y$

Figure 6. EDS spectrum of the constituents present on the microstructure shown on figure 5.

Crucibles evaluation

A pouring operation was performed for every tested crucible material, in order to evaluate the crucible thermal-shock resistance and the behavior of the $Y_2O_3$ film during melting. Results are very similar in every case, meaning that thermal-shock resistance is similar no matter the $ZrO_2$ stabilizing compound that is used. No crucible was found to present cracks after melting or was destroyed during melting. In what concerns the behavior of the $Y_2O_3$ film, its performance was not affected by the crucible base material and an effective separation between the $ZrO_2$ crucible refractory and the molten alloy was always achieved, as can be concluded after the absence of Zr in solution.

After melting, the $Y_2O_3$ film remains present at the inside crucible wall, showing no cracks, suggesting that it could probably be reused on a second melt (Figure 7).



Figure 7. Portion of a $Y_2O_3$ partially stabilized $ZrO_2$ crucible with inside $Y_2O_3$ layer, after melting a Ti-48Al alloy. The $Y_2O_3$ film is still visible at the inside crucible wall, and no cracks are detected.

A SEM/EDS analysis was performed at the $Y_2O_3$ film, before and after melting. Figure 8 shows that the $Y_2O_3$ grains suffered a slight vitrification, as some of them are adherent and their edges become round after melting.



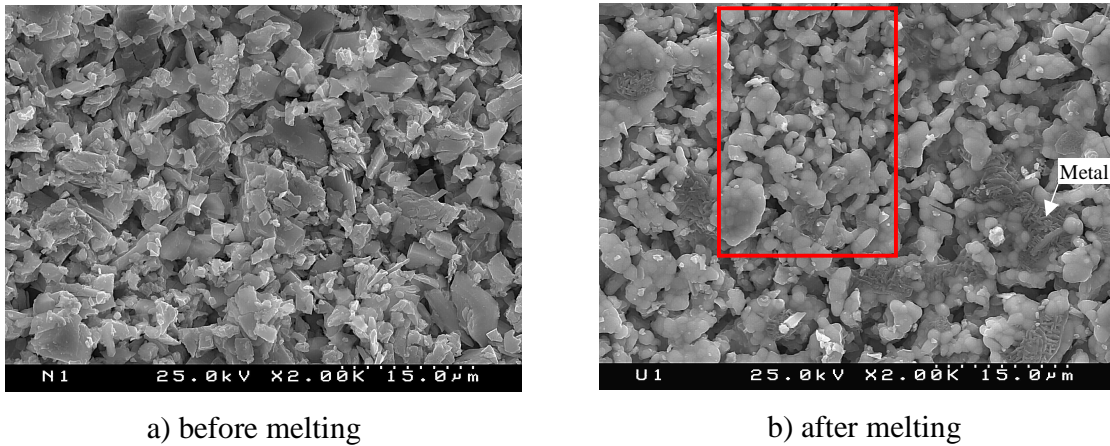| a) before melting | b) after melting |

Figure 8. $Y_2O_3$ film a) before melting and b) after melting/pouring a Ti-48Al alloy. A slight vitrification of yttria grains occurred, but there is no metal adherent to the refractory grains.

EDS spectrum performed in the area limited in figure 8 b) are shown in Figure 9, and reveal that besides yttrium oxide and the Ti-Al alloy, no other compound or element is present. On the other hand, Figure 8 b) shows that no metal-ceramic reaction occurred, and the molten alloy didn't wet the crucible wall, as the $Y_2O_3$ grains are clean, and only some Ti-Al fragments are mechanical entrapped between some ceramic grains.
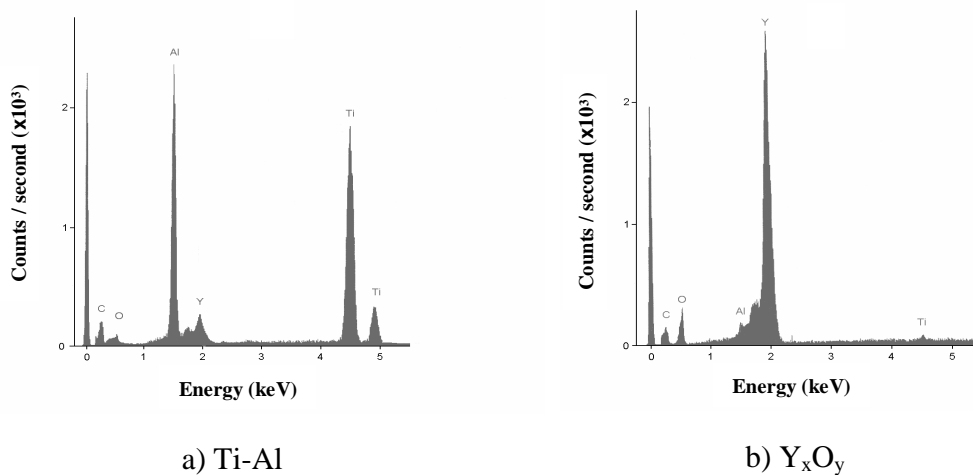


| a) Ti-Al | b) $Y_xO_y$ |

Figure 9. EDS spectrum of the constituents present on the microstructure shown on figure 8 b).

Final remarks

Figure 10 shows Ti-48Al samples obtained by melting in $Y_2O_3$ partially stabilized $ZrO_2$ crucible with inside $Y_2O_3$ layer, and cooled inside the crucible, and compares them with samples obtained in single $Y_2O_3$ partially stabilized $ZrO_2$ crucibles during previous experiments reported elsewhere [1, 5].

Besides the different surface finishing of the samples, revealing that an important metal-crucible interaction occurred when single $ZrO_2$ crucibles were used (Figure 10 a)), also the different shape of the samples top is different (Figure 10 b)) – concavous shape on the sample obtained in single $ZrO_2$ crucibles, suggesting a important metal-ceramic took place, and convex on samples obtained in this work, revealing that no reaction occurred.



a)                                              b)

Figure 10 – Comparison between Ti-48Al samples obtained in single and multi-layer $ZrO_2$ based crucibles, revealing different metal-crucible material interaction

## References

[1]   J. Barbosa, "Elaboração de Aluminetos de Titânio por Fusão de Indução em Cadinho Cerâmico e Vazamento em Moldação Cerâmica" (PhD thesis, University of Minho, Portugal, 2001).

[2]   C. Fruhe, D.R. Poirier, M.C. Maguire, R.A. Harding, "Attempts to develop a ceramic mould for titanium casting – a review", *International Journal of Cast Metals Research*, 9 (4) (1996), 233-240.

[3]   T. Sato, Y. Yoneda, N. Matsumoto, "A Technique for casting Titanium Alloys with Lime Refractory", *Proceedings of the 58th World Foundry Congress,* Cracow, Poland, 1991.

[4]   J. Barbosa, "Zr bearing γ-TiAl Induction Melted", *Key Engineering Materials*, 188

(2000), 45-54.

[5]   J. Barbosa et al., "Influence of Crucible Material on the Level of Contamination in TiAl Using Induction Melting", *International Journal of Cast Metals Research*, 12 (2000), 293-301.

[6]   J. Barbosa et al., "The Production of TiAl by Foundry Processes", *Key Engineering Materials*, 230-232 (2002), 106-109.

[7]   J. Barbosa et al., "Controlled Residual Surface Contamination of γ-TiAl, Induction Melted in Ceramic Crucible", *Proceedings of the Materials Week 2001 Congress*, Munich, Germany, October 2001.

[8]   R.L. Saha et al, "On the Evaluation of Stability of Rare Earth Oxides as Face Coats for Investment Casting of Titanium", *Metallurgical Transactions B*, 21B (1990), 559-566.

[9]   O.M.N.D.Teodoro, J.A.M.C. Silva and A.M.C. Moutinho, Vacuum 46 (1995), 1205.

[10]  Richerson et al, "Ceramic Composition and Crucibles and Molds Formed Therefrom" (U.S. Patent 4040845, 1997).

[11]  A. Menand et al., "Interstitial Solubility in γ and $\alpha_2$ Phases of TiAl Based Alloys", *Acta Materiallica*, 44 (12) (1996), 4729-4737.

[12]  T.S. Piwonka, "Reactions at the Mold/Metal Interface in Investment Castings", *Proceedings of the 42th Annual Technical Meeting of the Investment Casting Institute*", USA, 1994.